scientific reports

Check for updates

OPEN

Comparison of cytotoxicity effects induced by four different types of nanoparticles in human corneal and conjunctival epithelial cells

Xiangzhe Li[1,2], Boram Kang[1], Youngsub Eom[1], Jingxiang Zhong[2,3], Hyung Keun Lee[4], Hyo Myung Kim[1] & Jong Suk Song[1]✉

The impact of particulate matter (PM) on ocular surface health has attracted increased attention in recent years. Previous studies have reported that differences in the chemical composition of PM can affect the toxicological response. However, available information on the toxic effects of chemical components of PM on the ocular surface is insufficient. In this paper, we aimed to investigate the toxicity effects of chemical components of PM on the ocular surface, focusing on the effects of four different types of nanoparticles (NPs) in human corneal epithelial cells (HCECs) and human conjunctival epithelial cells (HCjECs), which include titanium dioxide (TiO_2), carbon black (CB), zinc dioxide (ZnO), and silicon dioxide (SiO_2). We found that the in vitro cytotoxic effects of CB, ZnO, and SiO_2 NPs are dependent on particle properties and cell type as well as the exposure concentration and time. Here, the order of increasing toxicity was SiO_2 → CB → ZnO, while TiO_2 demonstrated no toxicity. Moreover, toxic effects appearing more severe in HCECs than HCjECs. Reactive oxygen species (ROS)-mediated oxidative stress plays a key role in the toxicity of these three NPs in HCECs and HCjECs, leading to apoptosis and mitochondrial damage, which are also important contributors to aging. Sirtuin1 (SIRT1) as an NAD+-dependent protein deacetylase that seems to play a potential protective role in this process. These findings implied that ROS and/or SIRT1 may become a potential target of clinical treatment of PM- or NP-related ocular surface diseases.

Particulate matter (PM) is an important component of air pollution that affects ocular health[1]. A growing number of studies have shown that exposure to elevated PM concentrations is linked with an increased frequency of outpatient visits for ocular surface diseases, including nonspecific conjunctivitis, blepharitis, pterygium, and dry eye disease[2–5]. The chemical components of PM include mineral matter [e.g., oxides of aluminum (Al), calcium (Ca), titanium, silicon, zinc, iron (Fe), and magnesium (Mg), etc.], organic matter, elemental carbon, secondary inorganic aerosol, sea salt, and trace elements[6]. Previous studies have reported that the complex and variable composition of PM can lead to differences in health effects[7]. In particular, heavy metals are considered to contribute significantly to PM-related cytotoxicity[8]. However, few studies to date have focused on the different effects of these chemical components of PM on eyes.

A number of different types of nanoparticles (NPs), including titanium dioxide (TiO_2) NPs, carbon black (CB) NPs, and silicon dioxide (SiO_2) NPs, which can mimic different chemical components of PM, are often adopted in studies seeking to investigate the health effects of PM[9–14]. Oxidative stress plays an important role in the toxic effects of PM or NPs and has been extensively studied both in vitro and in vivo[15–20]. Previous studies have shown that both PM or NPs can increase the production of reactive oxygen species (ROS) and apoptosis in in vivo cornea cells[19,21,22]. In addition, Gao et al. reported that PM can induce DNA damage and cell senescence in human corneal epithelial cells (HCECs)[23]. It is well known that DNA damage, cellular senescence, and mitochondrial dysfunction as well as the production of ROS or inflammation are hallmarks of aging[24]. Recently, studies have shown that PM or SiO_2 NPs can damage human pulmonary fibroblast cells or bronchial epithelial

[1]Department of Ophthalmology, Guro Hospital, Korea University College of Medicine, 80, Guro-dong, Guro-gu, Seoul 152–703, South Korea. [2]Department of Ophthalmology, First Affiliated Hospital of Jinan University, Guangzhou, China. [3]Department of Ophthalmology, Sixth Affiliated Hospital of Jinan University, Dongguan, China. [4]Institute of Vision Research, Department of Ophthalmology, Yonsei University College of Medicine, Seoul, South Korea. ✉email: crisim@korea.ac.kr

Particle	Supplier	Material code	Size
TiO_2	Sigma-Aldrich Corp. (St. Louis, MO, USA)	#634662	< 100 nm
CB	Orion Engineered Carbons (Piscataway, NJ, USA)	Printex55	25 nm
ZnO	Sigma-Aldrich Corp. (St. Louis, MO, USA)	#544906	< 100 nm
SiO_2	Sigma-Aldrich Corp. (St. Louis, MO, USA)	#637238	10–20 nm

Table 1. Parameters of the four NPs.

cells through attenuates the expression of sirtuin1 (SIRT1)[25,26]. SIRT1 is an NAD+-dependent protein deacetylase that has been linked to various physiological and pathological processes and conditions, including DNA repair, aging, cellular senescence, oxidative stress, inflammation, and mitochondrial function[27–31]. Therefore, in the field of aging mechanisms and intervention, SIRT1 has been a topic of interest in recent years. However, the role of SIRT1 in ocular surface injury induced by PM or NPs remains unclear.

To evaluate the different effects of chemical components of PM on the ocular surface, this study conducted a systematic and comparative investigation of the toxicity effects of four different NPs (TiO_2, CB, ZnO, and SiO_2) on HCECs and human conjunctival epithelial cells (HCjECs). The toxic effects of these NPs on HCECs and HCjECs were investigated. In addition, the expression of SIRT1 as well as ROS generation, apoptosis, and mitochondrial function were investigated.

Materials and methods

Reagents. Keratinocyte-serum free medium (K-SFM), keratinocyte supplements containing human recombinant epidermal growth factor (EGF) and bovine pituitary extract, phenol red-free Dulbecco's modified Eagle medium, 0.05% Trypsin-ethylenediaminetetraacetic acid, fetal bovine serum, 1 × phosphate-buffered saline (PBS), and penicillin–streptomycin (10,000 U/mL) were purchased from Thermo Fisher Scientific (Waltham, MA, USA). Roswell Park Memorial Institute (RPMI)-1640 medium and bovine serum albumin (BSA) were obtained from Sigma-Aldrich Corp. (St. Louis, MO, USA). Fibronectin was purchased from Corning (Corning, NY, USA). Rat tail collagen type I was obtained from Advanced BioMatrix (San Diego, CA, USA). Water-soluble tetrazolium salt (WST)-8 cell viability kit was purchased from DoGen Bio (Seoul, Korea). The ApopTag Red in situ apoptosis detection kit was obtained from Millipore Sigma (Burlington, MA, USA). The tetramethylrhodamine ethyl ester (TMRE) mitochondrial membrane potential (MMP) assay kit (#ab113852) and 2′,7′-dichlorofluorescein diacetate (DCFH-DA) cellular ROS detection assay kit (#ab113851) were purchased from Abcam (Cambridge, England). Radioimmunoprecipitation assay buffer (#89901) was obtained from Thermo Fisher Scientific. Anti-SIRT1 (#8469) and β-actin (#5125) antibodies were purchased from Cell Signaling Technology (Danvers, MA, USA). Anti-mouse immunoglobulin G horseradish peroxidase–linked antibody (#PI-2000) was obtained from Vector Laboratories (Burlingham, NY, USA). Finally, eight-well black cell culture slides, 96-well black plates, and six-well and 96-well cell culture plates were purchased from SPL Life Sciences (Pocheon, Korea).

Particle preparation. Manufactured TiO_2, CB, ZnO, and SiO_2 NPs were purchased from the commercial suppliers indicated in Table 1. All particle samples were weighted on a high precision microbalance and a stock suspension was performed in sterile PBS at a concentration of 10 mg/mL. Prior to dilution in cell culture media, these suspensions were sonicated four times intermittently (for five minutes every 10 min) through a bath sonicator, then additionally sonicated three times for 20 s within 5 min prior to their experimental use so as to minimize their aggregation.

Cell culture and treatment. HCECs (2.040 pRSV-T, CRL-11516™) and HCjECs (clone 1-5c-4 [Wong-Kilbourne derivative (D) of Chang conjunctiva], KCLB No. 30052) were obtained from the American Type Culture Collection (ATCC; Manassas, VA, USA) and Korean Cell Line Bank (KCLB, Seoul, Korea), respectively. The HCECs were maintained in K-SFM supplemented with 0.05 mg/mL of bovine pituitary extract, 5 ng/mL of EGF, 100 U/mL of penicillin, and 100 µg/mL of streptomycin at 37 °C in a 5% CO_2 incubator. The flasks used were precoated overnight in a 37 °C incubator, using a mixture of 0.01 mg/mL of fibronectin, 0.03 mg/mL of bovine collagen type I, 0.01 mg/mL of BSA), and RPMI-1640. Before this step, the coating solution was discarded, and the flasks were kept in a biosafety hood for 15 min at room temperature. The HCjECs were maintained in RPMI-1640 containing 10% fetal bovine serum, 100 U/mL of penicillin, and 100 µg/mL of streptomycin at 37 °C in a 5% CO_2 incubator.

For experiments, HCECs (2×10^5 cells/mL) and HCjECs (2×10^5 cells/mL) were seeded in 96-well, 24-well, and six-well plates with 100 µL, 500 µL, and 2500 µL of culture medium, respectively. Cells were incubated for 24 h to reach 90% confluency and treated with NPs at the indicated concentration. The cellular responses were examined after first exposure and the results compared with those of untreated cells (control group).

Cytotoxicity tests. Cytotoxicity was evaluated using a WST-8 cell viability assay kit. The cells were incubated with or without different concentrations of each NP (12.5, 25, 50, 100, 200, or 400 µg/mL) for 24 h. The WST-8 solution (DoGen Bio, Seoul, Korea) was added to each well and cells were incubated for two hours; then, the colored supernatants were measured at 450 nm. The results are presented as percentages relative to the untreated control. All experiments were performed in triplicate.

In addition, to evaluate cytotoxicity with different exposure times, cells were incubated with each NP for 1, 3, 6, and 24 h with a relatively high concentration of 100 μg/mL. The half-maximal inhibitory concentration 50 (IC_{50}), or the concentration of NPs at which 50% of cells were nonviable, was determined. Data are presented as average IC_{50} values for each test NP, respectively.

Cellular uptake or interaction with NPs. The degree of NPs uptake or adsorption on cellular membranes was examined by analyzing forward scatter (FSC) verses side scatter (SSC) using flow cytometry (LSR-Fortessa X-20 program (BD Biosciences, San Jose, CA, USA) as described previously[32]. Briefly, cells were treated with 100 μg/mL of each NPs for 6 h, and then trypsinized and suspended in PBS for flow cytometry. Following gating, control and NPs-exposed cells were run and plotted to examine increase in side scatter (SSC) due to endocytotic or adsorptive NPs interaction.

Intracellular generation of ROS. DCFH-DA was used to measure intracellular ROS using the DCFH-DA cellular ROS detection assay kit according to the manufacturer's protocol. Cells were treated with 100 μg/mL of each NP for 3 h. Diluted DCFH-DA (10 μM) was then added to the cells, which were subsequently incubated for 30 min in the dark. A total of 10,000 events (cells) were analyzed by flow cytometry using the LSRFortessa X-20 program (BD Biosciences, San Jose, CA, USA) at excitation/emission wavelengths of 488/535 nm. The results were expressed as percentages of increase over control cells (as 100%).

Cell apoptosis analysis. Cells were seeded on cover slips in eight-well black cell culture slides and cultured overnight to allow for attachment. After exposure to 100 μg/mL of each NP for 6 h, the apoptotic cell count was detected using the TUNEL kit (ApopTag Red in situ apoptosis detection kit) according to the manufacturer's instructions. The cell nuclei were stained with 4′,6-diamidino-2-phenylindole. Images were captured with the LSM 700 laser scanning confocal microscope (Carl Zeiss, Jena, Germany). The percentage of TUNEL-positive cells was calculated in the total cells of each digital image (scale bar = 50 μm) of each group.

Detection of MMP. Cells were seeded in 96-well black plates and cultured overnight to allow for attachment. After exposure to 100 μg/mL of each NP for 6 h, the MMP was assessed using the TMRE assay. Cells were incubated for 30 min with TMRE at 500 nM diluted in warm culture medium at 37 °C and 5% CO_2. Cells were then washed twice with warm PBS/0.2% BSA and fluorescence intensity was detected using a plate reader with excitation/emission wavelengths at 549/575 nm.

Protein extraction and western blotting. Cells were seeded in six-well plates and cultured overnight to allow for attachment. After exposure to 100 μg/mL of each NP for 6 h, cells were lysed in radioimmunoprecipitation assay buffer for 30 min on ice. Protein concentrations were determined using the bicinchoninic acid method. Proteins were separated by 8% polyacrylamide gel electrophoresis containing 0.1% sodium dodecyl sulfate and transferred to polyvinylidene difluoride membranes. The nitrocellulose membrane was blocked with 5% BSA and subsequently incubated with SIRT1 monoclonal antibody (1:1000 dilution) overnight at 4 °C. Then, the membranes were incubated with horseradish peroxidase-conjugated horse anti-mouse immunoglobulin G secondary antibody (1:2000 dilution) for another hour. β-actin (1:10,000 dilution) was used as the loading control, and the ImageJ software (National Institutes of Health, Bethesda, MD, USA) was used to calculate protein intensity. The results of Western blot analysis were expressed as a ratio to β-actin, as previously described[10–13].

Statistical analyses. All data were expressed as the mean ± standard deviation (SD) values of at least three independent experiments. Statistical analyses were performed using one-way analysis of variance with post-hoc Tukey's test using the Statistical Package for Social Sciences version 20.0 program (IBM Corp., Armonk, NY, USA). Results were considered statistically significant at a p-value of less than 0.05.

Results

Cytotoxicity induced by NPs. We studied and compared the toxicity effects of four NPs in HCECs and HCjECs two cell lines. As expected, we found that cell toxicity is dependent on exposure concentration, particle properties, and cell type. The order of increasing toxicity of the tested NPs was $SiO_2 \rightarrow CB \rightarrow ZnO$. After 24 h of exposure at varying doses (12.5, 25, 50, 100, 200, and 400 μg/mL) of TiO_2, CB, ZnO, and SiO_2 NPs, the cell viability of HCECs and HCjECs as detected by the WST-8 assay resulted in explicit dose-dependent reductions, excluding TiO_2 NPs (Fig. 1A,B). Especially, ZnO NPs were shown to impart significant ($p < 0.001$) greater toxicity than the control treatment on both HCECs and HCjECs, even at the lowest dose (12.5 μg/mL), with IC_{50} values of 5.169 and 6.212 μg/mL, respectively (Fig. 1A,B). Conversely, toxicity with TiO_2 NPs was not observed in either cell line even with at the highest dose (400 μg/mL) (Fig. 1A,B). Meanwhile, HCECs were shown to be more susceptible to CB NPs than HCjECs in that the concentration of CB NPs able to cause toxicity in HCECs (25 μg/mL) was lower than that for HCjECs (50 μg/mL), with IC_{50} values of 89.89 and 222.9 μg/mL, respectively (Fig. 1A,B). The concentration of SiO_2 NPs causing toxicity in HCECs (100 μg/mL) was also lower than that for HCjECs (400 μg/mL), with IC_{50} values of 206.6 and 399.5 μg/mL, respectively (Fig. 1A,B).

In addition, we investigated the toxicity effects of NPs at the concentration of 100 μg/mL at different time points (1, 3, 6 and 24 h). The viability of HCECs and HCjECs resulted in an explicit time-dependent reduction, excluding TiO_2 NPs (Fig. 1C,D). The toxicity of CB and ZnO NPs on HCECs and HCjECs could be observed as early as 1 h after treatment (Fig. 1C,D). However, that of SiO_2 NPs was only observed in HCECs after 3 h after first exposure, and there were no toxic effects of SiO_2 NPs on HCjECs, even after 24 h of exposure (Fig. 1C,D).

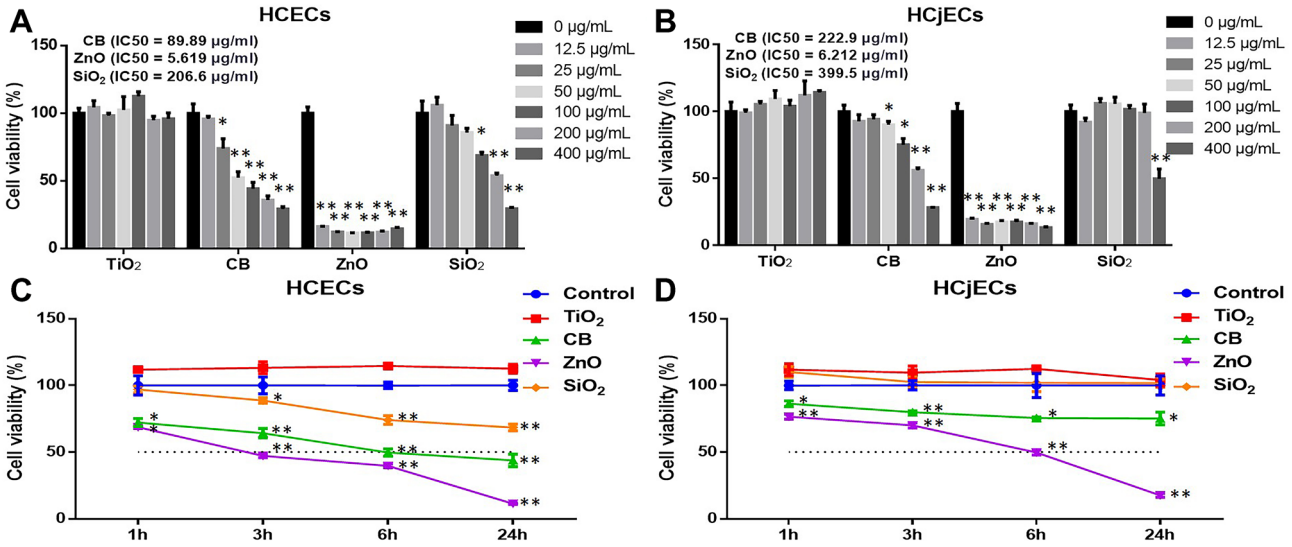

Figure 1. Cytotoxicity evaluation of TiO_2, CB, ZnO, and SiO_2 NPs with the WST-8 assay. HCECs (**A**) and HCjECs (**B**) were treated with different concentrations (12.5, 25, 50, 100, 200, or 400 µg/mL) of each NP for 24 h. The IC_{50} values of each NP are shown at the top left of A and B. In addition, HCECs (**C**) and HCjECs (**D**) were treated with 100 µg/mL of each NP for different lengths of time (1, 3, 6, and 24 h) and their viability was measured with the WST-8 assay. Results are given in percentages related to untreated control cells. Results are shown as the mean ± standard deviation values of three independent experiments, each of which was carried out in triplicate. *$p < 0.05$ and **$p < 0.001$ vs. untreated controls.

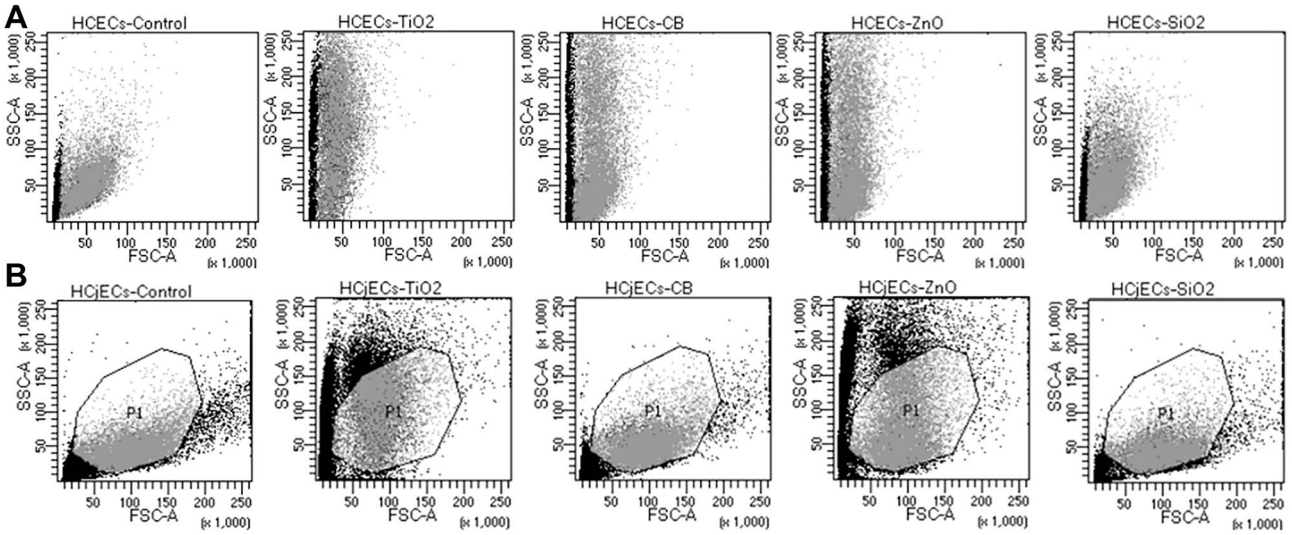

Figure 2. Analysis of NPs uptake was evaluated by analyzing FSC verses SSC using flow cytometry. HCECs (**A**) and HCjECs (**B**) were treated with 100 µg/mL of TiO_2, CB, ZnO, and SiO_2 NPs for 6 h. NPs uptake/surface adsorption is reflected by increases in the side scatter of cell populations (relative to controls).

In addition, ZnO NPs lessened cell viability by greater than 50% in HCECs (47.2%) and HCjECs (49.7%) after 3 and 6 h of exposure, respectively (Fig. 1C,D), while CB NPs did so in HCECs (49.7%) 6 h after first exposure, but cell viability in HCjECs remained at 75.2% even 24 h after first exposure to CB NPs (Fig. 1C,D). These results indicate that HCECs are more vulnerable to these NPs than HCjECs.

NPs uptake in HCECs and HCjECs. Uptake or attachment of NPs to cellular membranes in HCECs and HCjECs was examined by analyzing FSC verses SSC using flow cytometry. After 6 h of exposure to 100 µg/mL of the four NPs, we see that NPs had a variable effect on the side scatter of the cells, with all two cell types exhibiting substantial uptake or interaction with TiO_2 and ZnO NPs as evident by a large increase in side scatter/left shift (nanoparticle uptake-associate cell size reduction) (Fig. 2). In addition, CB NPs triggered substantial increase in side scatter compared to controls only in HCECs, but not in HCjECs (slight left shift) (Fig. 2). On the other hand, SiO_2 NPs triggered slight increase in side scatter compared to controls in both HCECs and HCjECs (Fig. 2).

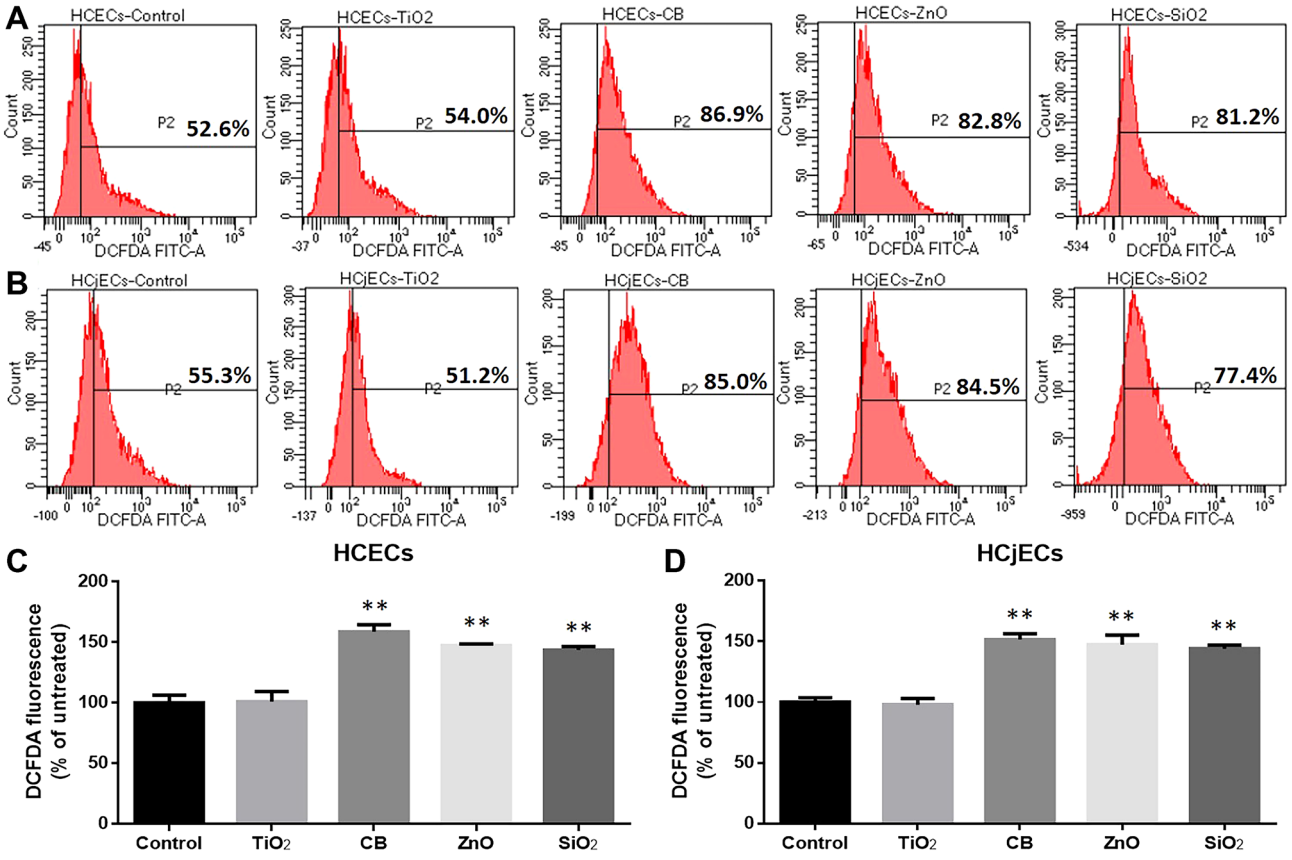

Figure 3. Intracellular ROS generation of cells was evaluated by DCFDH-DA oxidation assay. HCECs (**A**, **C**) and HCjECs (**B**, **D**) were treated with 100 μg/mL of TiO_2, CB, ZnO, and SiO_2 NPs for 3 h. The representative figures are shown, and DCFDA-positive cells (P2) were calculated as a percentage of the controls. Results are shown as the mean ± standard deviation values of three independent experiments, each of which was carried out in triplicate. *$p < 0.05$ and **$p < 0.001$ vs. untreated controls.

Intracellular ROS generation induced by NPs. ROS has been suggested to be an important biomarker in the evaluation of nanotoxicity[33]. We measured the production of intracellular ROS via DCFDH-DA oxidation assay, which is used to quantitatively assess ROS in live cell samples. Thus, we measured the ROS generation at an earlier time point (3 h) following exposure to NP (100 μg/mL). At this point, CB, ZnO, and SiO_2 NPs significantly increased the DCF fluorescence intensity relative to the control treatment in both HCECs and HCjECs. However, there were no significant changes in cells exposed to TiO_2 NPs (Fig. 3).

Apoptosis induced by NPs. Detection and quantification of apoptosis were carried out by TUNEL assay. Six hours after first exposure to 100 μg/mL of the four NPs, the percentage of TUNEL-positive cells were significantly ($p < 0.05$) increased in CB-exposed and ZnO-exposed cells relative to with control treatment among both HCECs and HCjECs (Fig. 4). However, SiO_2 NPs significantly ($p < 0.05$) increased apoptosis only among HCECs, not HCjECs (Fig. 4).

Changes in MMP induced by NPs. MMP was assessed using the TMRE assay. After 6 h of exposure to 100 μg/mL of the four NPs, TMRE fluorescence intensity was significantly decreased in CB-exposed and ZnO-exposed cells relative to among control cells in both HCECs and HCjECs ($p < 0.001$) (Fig. 5). However, SiO_2 NPs significantly reduced the TMRE fluorescence intensity only among HCECs ($p < 0.05$), not HCjECs (Fig. 5).

Changes in SIRT1 expression induced by NPs. SIRT1 expression was measured by western blotting in HCECs and HCjECs after exposure to 100 μg/mL of four NPs for 6 h. After NP exposure, SIRT1 expression was significantly decreased in CB-exposed and ZnO-exposed cells relative to after control treatment in both HCECs and HCjECs ($p < 0.05$) (Fig. 6). However, SiO_2 NPs significantly ($p < 0.05$) reduced SIRT1 expression only among HCECs, not HCjECs (Fig. 6).

Discussion

In recent years, the impact of PM on ocular surface health has attracted increased attention[1,34]. Previous studies have reported that differences in the chemical composition of PM can affect the toxicological response[35]. For example, Yuan et al. reported that heavy metals components such as Zn, chromium (Cr), manganese (Mn), Fe,

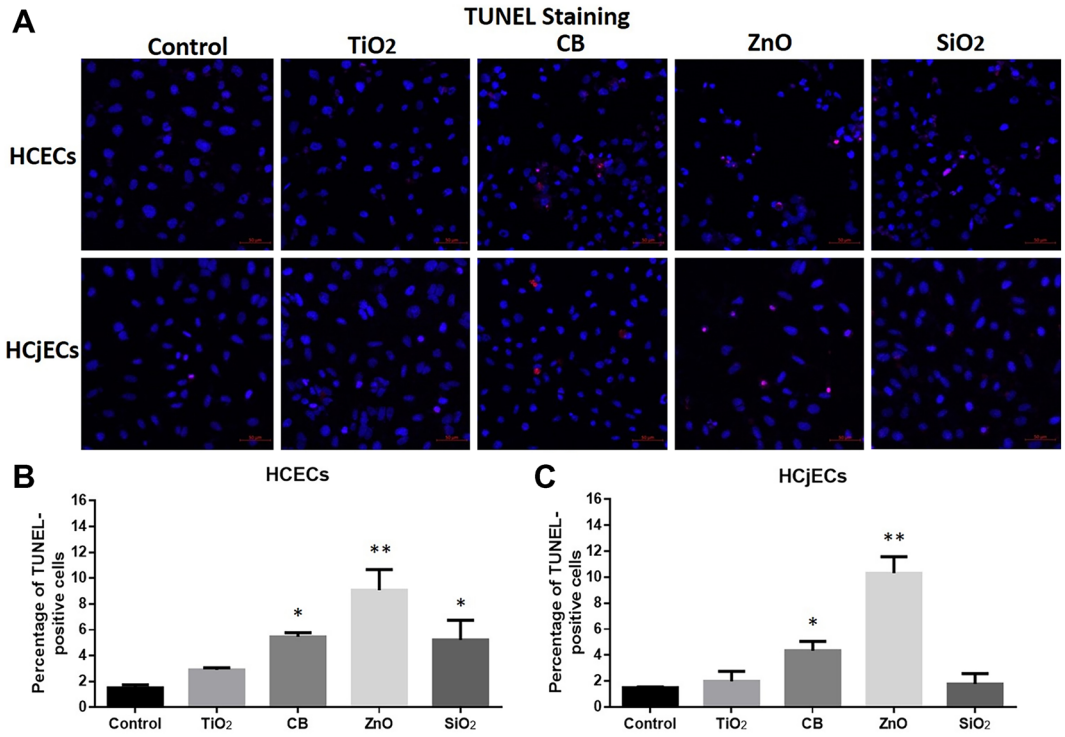

Figure 4. Cellular apoptosis was detected by TUNEL staining. (**A**) Representative TUNEL fluorescence images of HCECs and HCjECs treated with 100 μg/mL of TiO_2, CB, ZnO, and SiO_2 NPs for 6 h. (**B**) Percentage of TUNEL-positive cells in HCECs. (**C**) Percentage of TUNEL-positive cells in HCjECs. Cell nuclei are labeled with DAPI (blue) and TUNEL positive cells fluoresced red. Results are shown as the mean ± standard deviation values of three independent experiments, each of which was carried out in triplicate. *$p < 0.05$ and **$p < 0.001$ vs. untreated controls.

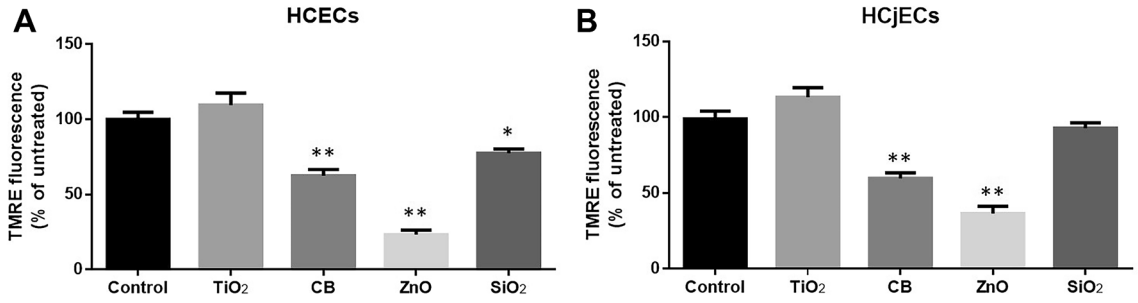

Figure 5. Mitochondrial membrane potential was measured by using the TMRE assay. HCECs (**A**) and HCjECs (**B**) were treated with 100 μg/mL of TiO_2, CB, ZnO, and SiO_2 NPs for 6 h. The results were calculated as a percentage of TMRE fluorescence intensity relative to controls. Results are shown as the mean ± standard deviation values of three independent experiments, each of which was carried out in triplicate. *$p < 0.05$ and **$p < 0.001$ vs. untreated controls.

copper (Cu), and lead (Pb) are considered to make a significant contribution to PM-related cytotoxicity in human lung epithelial cells[8]. However, available information on the toxic effects of chemical components of PM on the ocular surface is insufficient. NPs as surrogate particles for PM are widely used to explore the biological effects of PM. Previous studies have indicated that the cytotoxicity of NPs depends upon various factors such as cell type, particle properties, and exposure concentration and time[18,32,36]. Recently, Lee et al. evaluated the toxicity of five different types [silver (Ag), cerium dioxide (CeO_2), SiO_2, TiO_2, and ZnO] of NPs on rabbit cornea cells at different doses (1, 10, 12.5, 25, 50, and 100 μg/mL) for 24 hours[21]. These authors found that only Ag and ZnO NPs reduced cell viability following exposure at the highest concentration (100 μg/mL), while the other tested NPs had no toxicity effect on rabbit cornea cells[21]. However, the toxicity effects of TiO_2 and SiO_2NPs (treatment of 100 μg/mL for 24 h) have been shown by other in vitro studies, which evaluated such in mouse corneal endothelial cells and HCECs, respectively[14,22]. Thus, the cytotoxicity of NPs in the eye seems to highly depend on the cell type being considered.

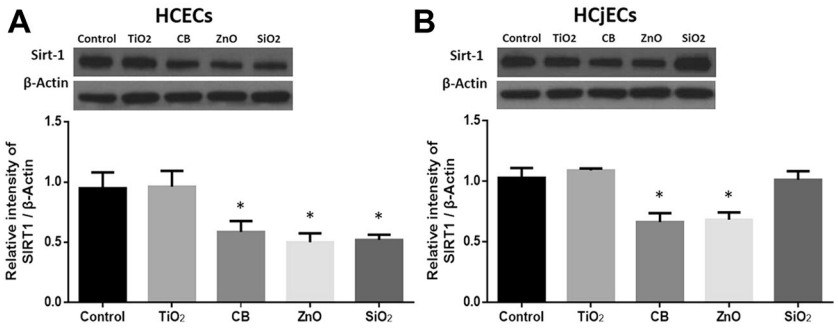

Figure 6. Expression of SIRT1 was evaluated by western blot analyses. HCECs (**A**) and HCjECs (**B**) were treated with 100 μg/mL of TiO_2, CB, ZnO, and SiO_2 NPs for 6 h. A representative example of a western blot gel image is shown at the top left of each figure (full length blot is presented in Supplementary Fig. 2). β-actin was used as an internal loading control. Results are expressed as a ratio to β-actin concentration and the mean ± standard deviation values of three independent experiments, each of which was carried out in triplicate. $^{*}p < 0.05$ and $^{**}p < 0.001$ vs. untreated controls.

This study evaluated the toxicity effect of four different NPs (TiO_2, CB, ZnO, and SiO_2) on cultured HCECs and HCjECs by cell viability assay and found that CB, ZnO, and SiO_2 NPs significantly reduced cell viability in a dose-dependent manner in both HCECs and HCjECs after 24 h exposure at varying doses of each NP. As shown by our results, the order of increasing toxicity of the tested NPs was SiO_2 → CB → ZnO. In addition, this study found that toxicity of CB and SiO_2 NPs on HCECs seems to be greater than that on HCjECs given that the IC_{50} value of these two NPs on HCjECs was twice as high as that on HCECs. However, the toxicity of ZnO NPs seems similar in two cell lines and is the greatest level of toxicity recorded in this study. Moreover, we evaluated the cytotoxicity of NPs at four different exposure times (1, 3, 6, and 24 h) using the concentration of 100 μg/mL and found that the toxicity induced by these NPs is also dependent on exposure time. Interestingly, 100 μg/mL of SiO_2 NPs was only toxic in HCECs, and the extent to which CB and ZnO NPs reduce cell viability over time was more obvious in HCECs than in HCjECs. Therefore, these results indicate that the toxic effects of NPs on both HCECs and HCjECs depend upon the particle properties and exposure concentration and time, which are consistent with the findings of a previous study involving rabbit cornea cells[21]. In addition, we found that the toxic effects of CB and SiO_2 NPs are highly dependent on the cell type in this study. However, if other NPs exhibit a high degree of toxicity like that of ZnO, the dependence of such on cell type seems to be weakened.

The generation of ROS and the subsequent production of oxidative stress is a predominant mechanism leading to nanotoxicity, including DNA damage, genotoxicity, apoptosis, and carcinogenesis[16,33,37,38]. In addition, mitochondria are the main site of cellular ROS production, and any structural and functional disorders can lead to mitochondrial ROS accumulation, which is the main inducer of apoptosis[39,40]. Therefore, to explore the role of oxidative stress in NP-induced cytotoxicity, this study evaluated ROS production, cell apoptosis, and mitochondrial membrane potential by using DCFDH-DA assay, TUNEL staining, and TMRE assay, respectively. On the other hand, ROS generation has been suggested to be an initial cellular response to NP internalization and, later, cell death[41]. Based on our toxicity test results, this study evaluated ROS as well as apoptosis and mitochondrial damage after 3 and 6 h of exposure, respectively. This study found that all positive NPs in the toxicity test induced ROS generation as well as apoptosis and mitochondrial damage when exposed to a dose of 100 μg/mL for 6 h. However, we found that SiO_2 NPs did not induce any cellular response in HCjECs, although there was an increase in ROS production. ROS play a dual role in the fate of cells, i.e., causing cell death as well as acting as second messengers to induce an adaptive cell response[42]. Interestingly, a recent study showed that SiO_2 NPs induce a slight increase of intracellular ROS but can activate mTOR and autophagy that avoids possible cellular damage induced by SiO_2 NPs[43]. Therefore, these results indicate that oxidative stress plays a key role in the properties and cell type–dependent toxicity of NPs, which is closely related to the production of ROS as well as potential defense mechanisms.

SIRT1, a member of the sirtuin family, is a highly conserved NAD + -dependent histone deacetylase and plays a crucial role in cell survival under oxidative stress conditions through directly regulating multiple targets, including eNOS, peroxisome proliferator-activated receptor-γ coactivator 1-α (PGC1α), p53, Forkhead Box O family (FoxO), and NF-Kb[44–49]. On the contrary, excessive ROS and/or oxidative stress conditions can inhibit the expression of SIRT1, thereby promoting cell apoptosis[30,50,51]. Previous studies have reported that exposure to NPs can inhibit the expression of SIRT1 to promote cell apoptosis, mitochondrial damage, and inflammation[26,52]. However, these injuries can be reversed by upregulating or activating SIRT1[26,52]. In this study, we found that all positive NPs in the toxicity test could reduce the expression of SIRT1 following exposure to a dose of 100 μg/mL for 6 h. However, we also found that SiO_2 did not reduce the expression of SIRT1 in HCjECs, although ROS production increased. Therefore, these results indicate that the expression of SIRT1 plays a potential protective role in the process of NP-induced, ROS-mediated oxidative stress, but excessive ROS can still inhibit the expression of SIRT1 to promote cell apoptosis and mitochondrial damage. It would be interesting to test whether the upregulation or activation of SIRT1 could reduce NP-induced oxidative stress in HCECs and HCjECs. Further studies are required to understand the protective mechanisms of SIRT1 on nanotoxicity in the eyes.

In conclusion, the results of the current study confirmed that the in vitro cytotoxic effects of CB, ZnO, and SiO_2 NPs are dependent on particle properties and cell type as well as the exposure concentration and time. In HCECs and HCjECs, ZnO NPs possessed the greatest toxicity, while TiO_2 NPs demonstrated no toxicity. We also showed that CB and SiO_2 NPs have different cytotoxic potencies in HCECs and HCjECs, while that of ZnO NPs was similar between the two cell types. HCECs seem to be more vulnerable to these NPs (as PM surrogate particles) than HCjECs. ROS-mediated oxidative stress plays a key role in the toxicity of NPs in HCECs and HCjECs, leading to apoptosis and mitochondrial damage. On the other hand, this study speculate that these NPs may promote aging effect to HCECs and HCjECs, as supported by the elevation of ROS production and mitochondrial damage as well as reduction of SIRT1 expression, which are indirect evidence to aging. SIRT1 seems to play a potential protective role in toxicity and aging-related effects of NPs to HCECs and HCjECs. In summary, our study provides evidence of a potential mechanism that may induce toxic and aging-related effects on the ocular surface induced by different chemical components of PM, through the use of four different types of NPs. These findings may provide valuable insights regarding the treatment of PM- or NP-related ocular surface injury in the future.

Received: 23 June 2021; Accepted: 1 December 2021
Published online: 07 January 2022

References

1. Jung, S. J., Mehta, J. S. & Tong, L. Effects of environment pollution on the ocular surface. *Ocul. Surf.* **16**, 198–205. https://doi.org/10.1016/j.jtos.2018.03.001 (2018).
2. Chang, C. J., Yang, H. H., Chang, C. A. & Tsai, H. Y. Relationship between air pollution and outpatient visits for nonspecific conjunctivitis. *Invest. Ophthalmol. Vis. Sci.* **53**, 429–433. https://doi.org/10.1167/iovs.11-8253 (2012).
3. Lee, K. W. *et al.* Outdoor air pollution and Pterygium in Korea. *J. Korean Med. Sci.* **32**, 143–150. https://doi.org/10.3346/jkms.2017.32.1.143 (2017).
4. Malerbi, F. K., Martins, L. C., Saldiva, P. H. & Braga, A. L. Ambient levels of air pollution induce clinical worsening of blepharitis. *Environ. Res.* **112**, 199–203. https://doi.org/10.1016/j.envres.2011.11.010 (2012).
5. Mo, Z. *et al.* Impacts of air pollution on dry eye disease among residents in Hangzhou, China: A case-crossover study. *Environ. Pollut.* **246**, 183–189. https://doi.org/10.1016/j.envpol.2018.11.109 (2019).
6. Terzi, E. *et al.* Chemical composition and mass closure of ambient PM10 at urban sites. *Atmos. Environ.* **44**, 2231–2239. https://doi.org/10.1016/j.atmosenv.2010.02.019 (2010).
7. Çakmak, G. *et al.* Investigation of spatial and temporal variation of particulate matter in vitro genotoxicity and cytotoxicity in relation to the elemental composition. *Mutat. Res. Genet. Toxicol. Environ. Mutag.* **842**, 22–34. https://doi.org/10.1016/j.mrgentox.2019.01.009 (2019).
8. Yuan, Y. *et al.* In vitro toxicity evaluation of heavy metals in urban air particulate matter on human lung epithelial cells. *Sci. Total Environ.* **678**, 301–308. https://doi.org/10.1016/j.scitotenv.2019.04.431 (2019).
9. Eom, Y. *et al.* Effect of titanium dioxide nanoparticle exposure on the ocular surface: An animal study. *Ocul. Surf.* **14**, 224–232. https://doi.org/10.1016/j.jtos.2015.12.003 (2016).
10. Eom, Y. *et al.* The effect of ambient titanium dioxide microparticle exposure to the ocular surface on the expression of inflammatory cytokines in the eye and cervical lymph nodes. *Invest. Ophthalmol. Vis. Sci.* **57**, 6580–6590. https://doi.org/10.1167/iovs.16-19944 (2016).
11. Han, J. Y., Kang, B., Eom, Y., Kim, H. M. & Song, J. S. Comparing the effects of particulate matter on the ocular surfaces of normal eyes and a dry eye rat model. *Cornea* **36**, 605–610. https://doi.org/10.1097/ICO.0000000000001171 (2017).
12. Li, X. *et al.* The protective effect of a topical mucin secretagogue on ocular surface damage induced by airborne carbon black exposure. *Invest. Ophthalmol. Vis. Sci.* **60**, 255–264. https://doi.org/10.1167/iovs.18-25964 (2019).
13. Li, X. *et al.* The protective effect of an eye wash solution on the ocular surface damage induced by airborne carbon black exposure. *Cornea* **39**, 1040–1047. https://doi.org/10.1097/ICO.0000000000002304 (2020).
14. Sun, D. *et al.* Toxicity of silicon dioxide nanoparticles with varying sizes on the cornea and protein corona as a strategy for therapy. *Sci. Bull.* **63**, 907–916. https://doi.org/10.1016/j.scib.2018.05.037 (2018).
15. Hyun, S.-W., Song, S. J., Park, B., Lee, T. G. & Kim, C.-S. Toxicological effects of urban particulate matter on corneal and conjunctival epithelial cells. *Toxicol. Res.* **36**, 311–318. https://doi.org/10.1007/s43188-019-00034-0 (2020).
16. Manke, A., Wang, L. & Rojanasakul, Y. Mechanisms of nanoparticle-induced oxidative stress and toxicity. *Biomed. Res. Int.* **2013**, 942916. https://doi.org/10.1155/2013/942916 (2013).
17. Sharma, V., Singh, P., Pandey, A. K. & Dhawan, A. Induction of oxidative stress, DNA damage and apoptosis in mouse liver after sub-acute oral exposure to zinc oxide nanoparticles. *Mutat. Res.* **745**, 84–91. https://doi.org/10.1016/j.mrgentox.2011.12.009 (2012).
18. Yang, H., Liu, C., Yang, D., Zhang, H. & Xi, Z. Comparative study of cytotoxicity, oxidative stress and genotoxicity induced by four typical nanomaterials: The role of particle size, shape and composition. *J. Appl. Toxicol.* **29**, 69–78. https://doi.org/10.1002/jat.1385 (2009).
19. Yang, Q. *et al.* Effects of fine particulate matter on the ocular surface: An in vitro and in vivo study. *Biomed. Pharmacother.* **117**, 109177. https://doi.org/10.1016/j.biopha.2019.109177 (2019).
20. Yoon, S., Han, S., Jeon, K. J. & Kwon, S. Effects of collected road dusts on cell viability, inflammatory response, and oxidative stress in cultured human corneal epithelial cells. *Toxicol. Lett.* **284**, 152–160. https://doi.org/10.1016/j.toxlet.2017.12.012 (2018).
21. Lee, H. & Park, K. In vitro cytotoxicity of zinc oxide nanoparticles in cultured statens seruminstitut rabbit cornea cells. *Toxicol. Res.* **35**, 287–294. https://doi.org/10.5487/TR.2019.35.3.287 (2019).
22. Yang, J. *et al.* Toxic effect of titanium dioxide nanoparticles on corneas in vitro and in vivo. *Aging* **13**, 5020–5033. https://doi.org/10.18632/aging.202412 (2021).
23. Gao, Z. X. *et al.* Assessment of DNA damage and cell senescence in corneal epithelial cells exposed to airborne particulate matter (PM25) collected in Guangzhou, China. *Invest. Ophthalmol. Vis. Sci.* **57**, 3093–3102. https://doi.org/10.1167/iovs.15-18839 (2016).
24. Lopez-Otin, C., Blasco, M. A., Partridge, L., Serrano, M. & Kroemer, G. The hallmarks of aging. *Cell* **153**, 1194–1217. https://doi.org/10.1016/j.cell.2013.05.039 (2013).
25. Tien, C. P. *et al.* Ambient particulate matter attenuates Sirtuin1 and augments SREBP1-PIR axis to induce human pulmonary fibroblast inflammation: Molecular mechanism of microenvironment associated with COPD. *Aging* **11**, 4654–4671. https://doi.org/10.18632/aging.102077 (2019).
26. Zhao, X. *et al.* JNK activation-mediated nuclear SIRT1 protein suppression contributes to silica nanoparticle-induced pulmonary damage via p53 acetylation and cytoplasmic localisation. *Toxicology* **423**, 42–53. https://doi.org/10.1016/j.tox.2019.05.003 (2019).

27. Chen, C., Zhou, M., Ge, Y. & Wang, X. SIRT1 and aging related signaling pathways. *Mech. Ageing Dev.* **187**, 111215. https://doi.org/10.1016/j.mad.2020.111215 (2020).
28. Chen, Z., Shentu, T. P., Wen, L., Johnson, D. A. & Shyy, J. Y. Regulation of SIRT1 by oxidative stress-responsive miRNAs and a systematic approach to identify its role in the endothelium. *Antioxid. Redox. Signal* **19**, 1522–1538. https://doi.org/10.1089/ars.2012.4803 (2013).
29. Horio, Y., Hayashi, T., Kuno, A. & Kunimoto, R. Cellular and molecular effects of sirtuins in health and disease. *Clin. Sci.* **121**, 191–203. https://doi.org/10.1042/CS20100587 (2011).
30. Salminen, A., Kaarniranta, K. & Kauppinen, A. Crosstalk between oxidative stress and SIRT1: Impact on the aging process. *Int. J. Mol. Sci.* **14**, 3834–3859. https://doi.org/10.3390/ijms14023834 (2013).
31. Zhou, M., Luo, J. & Zhang, H. Role of Sirtuin 1 in the pathogenesis of ocular disease (review). *Int. J. Mol. Med.* **42**, 13–20. https://doi.org/10.3892/ijmm.2018.3623 (2018).
32. Sohaebuddin, S. K., Thevenot, P. T., Baker, D., Eaton, J. W. & Tang, L. Nanomaterial cytotoxicity is composition, size, and cell type dependent. *Part Fibre Toxicol.* **7**, 22. https://doi.org/10.1186/1743-8977-7-22 (2010).
33. Fu, P. P., Xia, Q., Hwang, H. M., Ray, P. C. & Yu, H. Mechanisms of nanotoxicity: Generation of reactive oxygen species. *J. Food Drug. Anal.* **22**, 64–75. https://doi.org/10.1016/j.jfda.2014.01.005 (2014).
34. Lyu, D. *et al.* Transcriptomic profiling of human corneal epithelial cells exposed to airborne fine particulate matter (PM2.5). *Ocul. Surf.* **18**, 554–564. https://doi.org/10.1016/j.jtos.2020.06.003 (2020).
35. Ronkko, T. J. *et al.* Emissions and atmospheric processes influence the chemical composition and toxicological properties of urban air particulate matter in Nanjing, China. *Sci. Total Environ.* **639**, 1290–1310. https://doi.org/10.1016/j.scitotenv.2018.05.260 (2018).
36. Mironava, T., Hadjiargyrou, M., Simon, M., Jurukovski, V. & Rafailovich, M. H. Gold nanoparticles cellular toxicity and recovery: Effect of size, concentration and exposure time. *Nanotoxicology* **4**, 120–137. https://doi.org/10.3109/17435390903471463 (2010).
37. Kumar, A. & Dhawan, A. Genotoxic and carcinogenic potential of engineered nanoparticles: An update. *Arch. Toxicol.* **87**, 1883–1900. https://doi.org/10.1007/s00204-013-1128-z (2013).
38. Rim, K. T., Song, S. W. & Kim, H. Y. Oxidative DNA damage from nanoparticle exposure and its application to workers' health: A literature review. *Saf. Health Work* **4**, 177–186. https://doi.org/10.1016/j.shaw.2013.07.006 (2013).
39. El-Osta, H. & Circu, M. L. in *Mitochondrial Mechanisms of Degeneration and Repair in Parkinson's Disease* (ed Lori M. Buhlman) 1–23 (Springer, 2016).
40. Hekimi, S., Wang, Y. & Noe, A. Mitochondrial ROS and the effectors of the intrinsic apoptotic pathway in aging cells: The discerning killers!. *Front. Genet.* **7**, 161. https://doi.org/10.3389/fgene.2016.00161 (2016).
41. Long, T. C. *et al.* Nanosize titanium dioxide stimulates reactive oxygen species in brain microglia and damages neurons in vitro. *Environ. Health Perspect.* **115**, 1631–1637. https://doi.org/10.1289/ehp.10216 (2007).
42. Suzuki, Y. J., Forman, H. J. & Sevanian, A. Oxidants as stimulators of signal transduction. *Free Radical Biol. Med.* **22**, 269–285. https://doi.org/10.1016/S0891-5849(96)00275-4 (1997).
43. Park, J. H. *et al.* The effect of silica nanoparticles on human corneal epithelial cells. *Sci. Rep.* **6**, 37762. https://doi.org/10.1038/srep37762 (2016).
44. Brunet, A. *et al.* Stress-dependent regulation of FOXO transcription factors by the SIRT1 deacetylase. *Science* **303**, 2011–2015. https://doi.org/10.1126/science.1094637 (2004).
45. Luo, J. *et al.* Negative control of p53 by Sir2alpha promotes cell survival under stress. *Cell* **107**, 137–148. https://doi.org/10.1016/s0092-8674(01)00524-4 (2001).
46. Mattagajasingh, I. *et al.* SIRT1 promotes endothelium-dependent vascular relaxation by activating endothelial nitric oxide synthase. *Proc. Natl. Acad. Sci. USA* **104**, 14855–14860. https://doi.org/10.1073/pnas.0704329104 (2007).
47. Rodgers, J. T. *et al.* Nutrient control of glucose homeostasis through a complex of PGC-1alpha and SIRT1. *Nature* **434**, 113–118. https://doi.org/10.1038/nature03354 (2005).
48. Vaziri, H. *et al.* hSIR2(SIRT1) functions as an NAD-dependent p53 deacetylase. *Cell* **107**, 149–159. https://doi.org/10.1016/s0092-8674(01)00527-x (2001).
49. Yeung, F. *et al.* Modulation of NF-kappaB-dependent transcription and cell survival by the SIRT1 deacetylase. *EMBO J.* **23**, 2369–2380. https://doi.org/10.1038/sj.emboj.7600244 (2004).
50. Li, H., Bai, Z., Li, C., Sheng, C. & Zhao, X. EV71 infection induces cell apoptosis through ROS generation and SIRT1 activation. *J. Cell Biochem.* **121**, 4321–4331. https://doi.org/10.1002/jcb.29628 (2020).
51. Zhao, X. *et al.* Promotion of SIRT1 protein degradation and lower SIRT1 gene expression via reactive oxygen species is involved in Sb-induced apoptosis in BEAS-2b cells. *Toxicol. Lett.* **296**, 73–81. https://doi.org/10.1016/j.toxlet.2018.07.047 (2018).
52. Duan, W. X. *et al.* NiO nanoparticles induce apoptosis through repressing SIRT1 in human bronchial epithelial cells. *Toxicol. Appl. Pharmacol.* **286**, 80–91. https://doi.org/10.1016/j.taap.2015.03.024 (2015).

Acknowledgements

This research was supported by the Basic Science Research Program through the National Research Foundation of Korea (NRF), funded by the Ministry of Education (NRF-2017R1D1A1B03028552, 2019R1A2C1088904). The funding organization had no role in the design or conduct of this research.

Author contributions

X.Z.L.: Methodology, formal analysis, and writing–original draft preparation.B.-R.K. and Y.E.: Supervision and data curation.J.X.Z. and H.K.L.: Investigation and laboratory data analysis.H.M.K.: Formal analysis.J.S.S. (corresponding authors): Conceptualization, supervision, and project administration.

Competing interests

The authors declare no competing interests.

Additional information

Supplementary Information The online version contains supplementary material available at https://doi.org/10.1038/s41598-021-04199-3.

Correspondence and requests for materials should be addressed to J.S.S.

Reprints and permissions information is available at www.nature.com/reprints.

Publisher's note Springer Nature remains neutral with regard to jurisdictional claims in published maps and institutional affiliations.